

INFRARED THERMOMETERS: THEORY AND CONSTRUCTION

Infrared thermometers (IRTs) measure the energy radiated from the object whose temperature is being measured. Thus the IRT can measure this radiation from a distance. There need be no contact between the thermometer and the object because, unlike thermocouples, RTD's, and filled system bulbs, the IRT need not be at the same temperature as the object being measured. IRTs are suited especially to the measurement of moving or contact sensitive objects, objects inside vacuum or pressure vessels, or in hazardous locations, e.g. nuclear radiation environments. The speed of response of even slower types of IRTs is usually less than 1 second. Many respond in a few milliseconds.

Although the simplest IRTs are rugged and may be in service for decades, they require routine maintenance to keep the sighting path clear and to keep optical elements clean. The sophisticated IRTs needed for difficult problems of temperature measurement have complicated optics, some with rotating or moving parts, and usually have electronic signal conditioners.

Lastly, the advantageous results of using IRTs to solve difficult temperature measurements are frequently obtained only after significant engineering investigation of a particular application to select the optimum radiation and to install it in a way that yields a reliable measurement of product temperature.

ATMOSPHERIC ABSORPTION

IRTs differ from most other temperature sensors in that the sight path between the sensor and the object being measured is part of the measurement equation. The transmission of infrared radiation through the atmosphere is affected by the absorption characteristics of the many constituents found in the atmosphere. The atmosphere is composed of gases, liquids, and solid particles, all of which attenuate or scatter infrared radiation in one way or another.

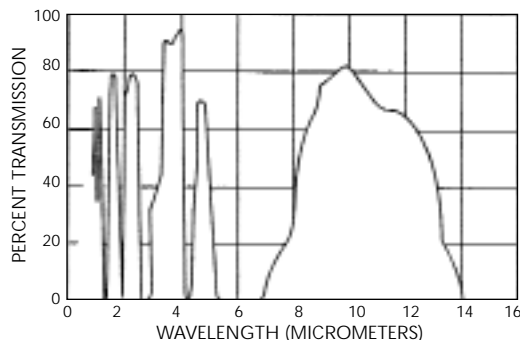


Fig. 1 Water Vapor Transmission Characteristics

About 78 percent of the air we breathe is nitrogen and 20 percent is oxygen; the rest consists of helium, argon, carbon dioxide, hydrogen, methane, neon, krypton, and ozone. Water Vapor (H_2O) is probably the single most important attenuator of infrared radiation. Major water vapor bands occur at 1.38, 1.87, 2.7, and 6.3 micrometers, (Fig.1). Most water vapor is near the surface of the earth.

Carbon dioxide (CO_2) and ozone (O_3) are two other major contributors to the attenuation of transmitted infrared energy. Carbon dioxide absorbs most strongly at 2.0, 2.7, 4.3, and 15.0 micrometers. Ozone bands absorb energy between 9.3 and 9.8 micrometers. Infrared instruments and systems should avoid all or most of the atmospheric absorption bands where practical, but if this is not possible in certain cases, calibration of the infrared system should take into account atmospheric path length and humidity.

TYPES OF INFRARED THERMOMETERS

The following is a convenient classification of IRTs:

- Broadband thermometers
- Band-pass thermometers
- Narrow band thermometers
- Ratio thermometers
- Fiber optic thermometers

BROADBAND THERMOMETERS

Broadband thermometers have usually been the simplest IRTs, with spectral responses from 0.3 microns wavelength to an upper limit of 2.5 to 20 microns (μm), determined by the lens or window material. They have been termed "total radiation" thermometers because, in the temperature ranges of normal use they measure a significant fraction of all the thermal radiation emitted by the object whose temperature is being measured.

BROADBAND:

Advantages

1. Economy
2. Wide temperature spans
3. Simple

Disadvantages

1. Lower sensitivity
2. Susceptible to absorption errors due to sight path conditions



Fig. 2 A Modern Infrared Thermometer

BAND-PASS THERMOMETERS

Band-pass thermometers were initially derived from simple, broadband thermometers. Lens, window, or filter characteristics were selected to view only a selected portion of the spectrum. The $5 \pm 0.2\mu\text{m}$ band-pass was used to measure glass surface temperature because glass emits strongly in this region, but poorly below or immediately above this band. However, an $8\text{-}14\mu\text{m}$ band-pass can be used to measure glass surface if the glass has surroundings cooler than itself. The $8\text{-}14\mu\text{m}$ band is also preferred for low temperature, general-purpose use because energy in this band is not attenuated by atmospheric moisture.

NARROW BAND THERMOMETERS

Narrow band thermometers operate over a narrow range of wavelengths. The spectral response of many narrow band thermometers is determined by the optical filter used. Such narrow band thermometers are used as general-purpose instruments over the temperature range of interest. For example, a thermometer using a silicon cell detector will have a response that peaks at $0.9\mu\text{m}$. The upper limit of usefulness is about $1.1\mu\text{m}$. Such a thermometer can only be used at temperatures above 600°C (1100°F).

Other narrow band thermometers utilize filters to restrict response to a selected wavelength to meet the needs of a particular application. Some examples are:

| Wavelength- μm | Application |
|---------------------------|--|
| 0.65 | Accurate measurement of high temperature objects in the open |
| 3.43 ± 0.2 | Thin film, polyethylene-type plastics |
| 3.86 | To measure through products of combustion |

NARROW BAND:

Advantages

1. High accuracy even when emissivity unknown or varying, if short wavelength units chosen. For measuring in the open
2. Selected wave-bands for looking at or through glass, plastics and flames.

Disadvantages

1. Narrow temperature spans
2. Difficult to select optimum unit to meet all criteria.

RATIO THERMOMETERS

A ratio thermometer measures radiated energy in two narrow bands and calculates the ratio of the two energies. This ratio is a temperature-dependent function. The temperature measurement is not primarily dependent on the energy in the two bands, only on the ratio of the two energies. Therefore, any influence that affects the amount of energy in each band by the same percentage has no effect on the temperature indication. Changes in target size have no effect. If the emissivity of the target is the same at both wavelengths, the indicated temperature is not changed by changes in emissivity. Unfortunately, this condition is not fulfilled by all oxidizable materials. For other materials, the ratio techniques may reduce or eliminate changes in indicated temperature caused by changes in surface finish. The ratio technique may reduce the effect of energy-absorbing materials such as particulates or CO_2 between the target and the thermometer, if the percentage of absorption is the same at each wavelength.

RATIO:

Advantages

1. Less sensitive to varying target size or intermittent blockage of sight path by smoke, particles, etc.

Disadvantages

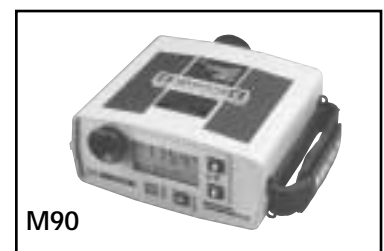
1. Higher cost
2. Need to know ratio of emissivity in the two wavebands of measurement.
3. Sensitive to changes in ratio of emissivities

OPTICAL PYROMETERS

Although optical pyrometers are no longer manufactured in significant numbers, there are probably hundreds of thousands in everyday use, and they are sufficiently unique in design and use to warrant a separate discussion.

An optical pyrometer measures the radiation from the target in a narrow band of visible wavelengths, centered at about $0.65 \mu\text{m}$ in the red/yellow portion of the spectrum. The most commonly used optical pyrometers are manually operated. The operator sights the pyrometer on the target. At the same time he can see in the eyepiece the image of an internal tungsten lamp filament.

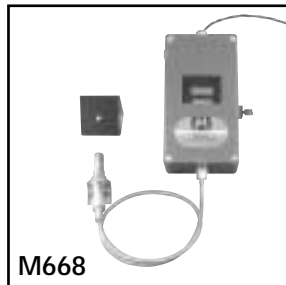
The operator matches the filament color to the target by varying the current through the filament with a rheostat, and when the target image and the tungsten filament image are the same color, the target temperature can



be read from a scale on the rheostat knob. When the target and filament colors are the same, the filament image apparently vanishes, so these pyrometers have also been called disappearing filament pyrometers.

FIBER OPTIC THERMOMETERS

In fiber optic thermometers, the infrared radiation from the target is guided to the detector by a light guide. The first such sensors used a 1/8 in. diameter sapphire rod to pick up energy from the target and transmit it to a detector. Contemporary fiber optics pyrometers use a flexible bundle of glass fibers with or without a lens. The spectral response of these fibers extends to about 2 μm , though some exotic materials such as fluorides have a wider band pass. Some are useful at target temperatures as low as 100°C (212°F).



Fiber optic thermometers are especially useful where

it is difficult, dangerous or impossible to obtain or maintain a clear sighting path to the target, as in pressure or vacuum chambers. Fiber optic thermometers have also been used to measure temperatures of turbine blades in gas turbines, and the temperature of small objects in induction heating coils.

THE THEORETICAL BASIS FOR RADIATION MEASUREMENTS

BLACKBODY RADIATION

All bodies radiate energy to their surroundings proportional to their absolute temperature. Although the emitted radiation of a body includes all wavelengths, the region in which the amount of radiation is significant to industrial temperature measurement extends from 0.3 μm to about 20 μm . From 0.4 μm to 0.7 μm is the visible region. Radiation at wavelengths longer than 0.7 μm is in the infrared region, which humans cannot see.

The thermal energy radiated by an object is expressed in relation to the energy radiated at the same temperature by a perfect radiator, traditionally called a blackbody. A blackbody absorbs all the radiation it

receives, and radiates more thermal radiation for all wavelength intervals than any other mass of the same area and temperature.

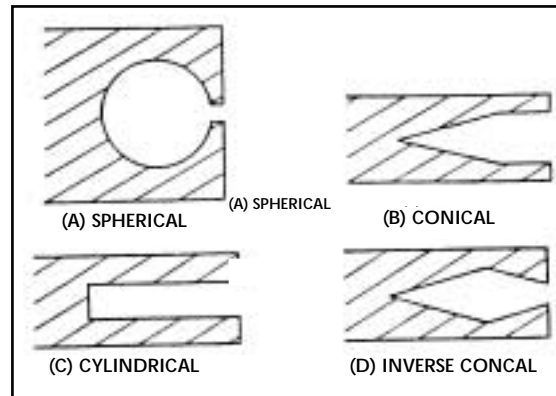


Fig. 3a Blackbody Cavities

Though the blackbody is an ideal, and no perfect blackbody exists, specially constructed laboratory sources emit radiation with an efficiency compared to a blackbody of 98% or higher. Laboratory sources with 99.98% efficiency compared to a blackbody have been constructed. The most common approach to realizing a blackbody is to use a spherical cavity with a small hole in the surface or a closed end tube that is longer than its diameter. The opaque walls of the sphere or tube are held at uniform temperature.

As shown in Fig. 3a, these constructions provide for multiple reflections of any radiation entering the opening. Thus, though the sphere or tube walls are slightly reflective, after many reflections all the energy is absorbed, i.e., at room temperature the aperture in the sphere or tube appears to be black in the visible part of the spectrum and is also nearly totally absorbing in other regions of the spectrum. At any given temperature the aperture radiates energy at nearly the same rate as a blackbody of the same size and temperature. Figure 3b illustrates a commercial secondary reference furnace based on a small opening in a uniformly heated spherical cavity.

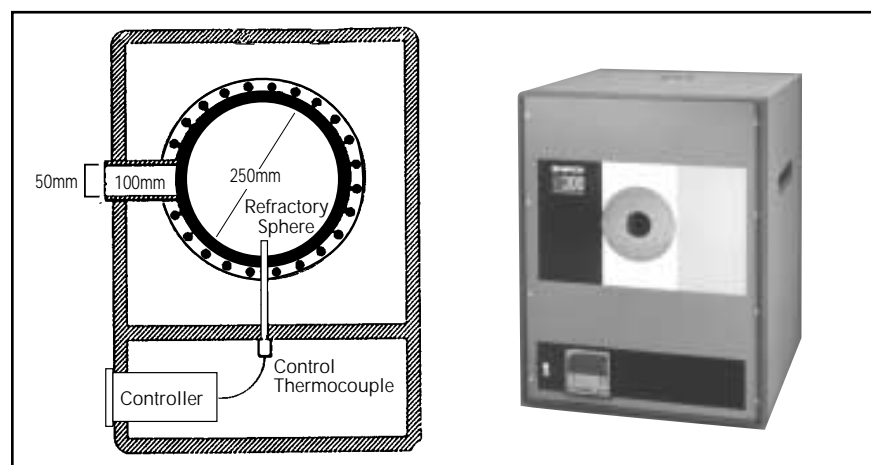


Fig. 3b Spherical Cavity Secondary Standard 200° to 1200°C

Another configuration used for a blackbody source is a deep wedge, where the cavity subtends only a small angle. Multiple reflections from the sides of the wedge make it appear black. The real importance of the wedge is conceptual. Surface roughness of an object can be visualized as a multitude of small wedges as in a machined surface or casting. If the surface is very rough, the

wedges are deep, and the object will have radiating properties that are closer to those of a blackbody than if the surface were smooth.



STEFAN-BOLTZMANN LAW

The rate at which a blackbody radiates energy is given by the Stefan-Boltzmann Law:

$$w = \sigma T^4$$

w = watts/meter²
 σ = Stefan-Boltzmann constant,
 5.6697×10^{-8} watts/m² - T
 T = Absolute temperature, kelvins

This equation assumes that the body receiving the radiation is at absolute zero. In the practical case, the receiving body is at a temperature T_R and radiates to the blackbody at a rate $w = \sigma T_R^4$ per unit area of the receptor. Thus, the net energy reaching the receptor is:

$$w = K\sigma(T^4 - T_R^4)$$

where K is a constant, taking into account the areas of the blackbody and receptor and the distance between them.

These equations give the radiation from all wavelengths in the entire spectrum. For more practical use, where the receiving object (the detector in a radiation thermometer, for example) responds significantly only to the short wavelength portion of the spectrum, the Wien-Planck and Wien Laws are more useful.

WIEN-PLANCK LAW

The Wien-Planck Law expresses the radiation emitted per unit area of a blackbody as a function of wavelength, λ , and temperature, T .

$$J_{\lambda T} d\lambda = C_1 \lambda^{-5} (\epsilon^{-C_2/\lambda T} - 1)^{-1} d\lambda$$

This function is plotted for several temperatures in Figure 4.

C_1 , the first radiation constant =
 3.7415×10^{-16} watts/m²

C_2 , the second radiation constant =
 1.43879×10^2 m·K

WIEN'S LAW

If λT is much greater than 1, the Wien-Planck Law can be approximated by Wien's Law.

$$J_{\lambda T} = C_1 \lambda^{-5} \epsilon^{-C_2/\lambda T}$$

This expression agrees with the Wien-Planck law within 1% if λT is less than 0.003 meter ·K (3000μm·K).

At 0.65 - μm wavelength, this condition exists for temperatures below 4600K. Therefore, Wien's Law has been commonly used with high accuracy in the field of optical pyrometry.

WIEN'S DISPLACEMENT LAW

In Fig. 4 it can be observed that as temperature increases, not only does the amount of radiation per unit area increase, but the wavelength at which the radiation is maximum shifts to shorter wavelengths.

The value of the wavelength of maximum radiation per unit area is given by Wien's Displacement Law.

$$\lambda_m T = b$$

λ_m = the wavelength of maximum radiation, meters

T = temperature, K

b = 2.8978×10^{-3} m·K

If λ is given in μm, $b = 2.8978 \times 10^3 \mu\text{m} \cdot \text{K}$. Referring to Fig. 4, at 2000°F (1366K) $\lambda_m = 2.1 \mu\text{m}$

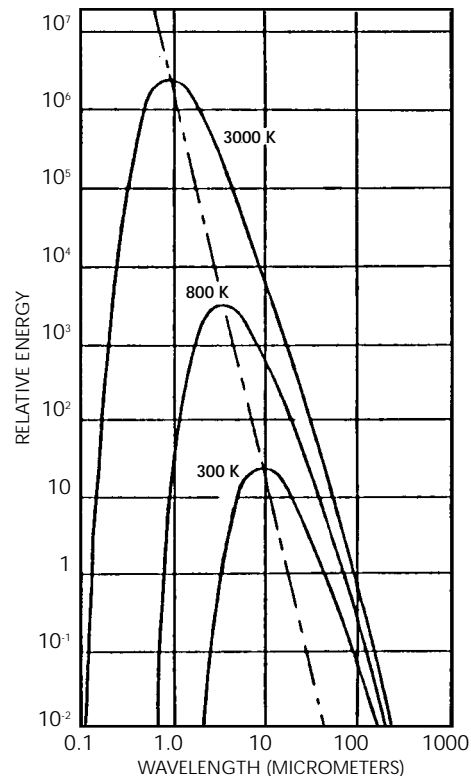


Fig. 4 Radiation Intensity as a Function of Wavelength and Temperature (Planck's Law)

NON-BLACKBODY RADIATION

The blackbody is an ideal concept. Real objects do not emit radiation as blackbodies, but at some lower rate. The ratio of the energy radiated by a body to that radiated by a blackbody at the same temperature is emittance (e), a number less than 1. If the body is opaque, the emittance (e) is related to the reflectance (r) of the body by:

$$e + r = 1 \text{ or } e = 1 - r$$

To understand that this must be true, consider an opaque object at temperature T , which is at equilibrium with its surroundings. This means that temperature T is not changing. Nearby bodies radiate energy according to their temperatures, some of which reaches the object. Some energy is reflected by the object. The remainder is absorbed. But the object is also emitting radiation proportional to its temperature, T . If the temperature is not changing, then the absorbed radiation must be balanced by the emitted radiation. If the emitted energy is greater than the absorbed energy, the object will cool. If the object absorbs more than it emits, the temperature will increase.

Thus, for any opaque body the emittance (e) equals the absorbance (a).

If the object is translucent, like some plastics or glass, some of the energy incident on the object will be transmitted through the object. Therefore, in general, t is transmittance, and

$$e + r + t = 1$$

For most materials, e , r , and t are functions of wavelength.

Fig. 5 illustrates the variation in emittance with wavelength for some materials. In general, the emittance of metals is highest at short wavelengths. The emittance of ceramics is highest at long wavelengths.

Because emittance is wavelength-dependent and the amount of energy radiated at each wavelength depends on temperature, the apparent emittance, also referred to as emissivity, of a material depends on the temperature at which it was determined, at the wavelengths at which the measurement is taken.

| | Total | Spectral 0.65-1.0 μ m |
|-------------------|-------------|---------------------------|
| Aluminum | | |
| Unoxidized | 0.02 - 0.15 | 0.05 - 0.25 |
| Lightly oxidized | 0.1 - 0.2 | 0.2 - 0.3 |
| Heavily oxidized | 0.3 - 0.4 | 0.4 |
| Chromium | | |
| Unoxidized | 0.08 - 0.2 | 0.3 - 0.6 |
| Lightly oxidized | 0.3 - 0.5 | 0.5 - 0.6 |
| Heavily oxidized | 0.8 | 0.7 - 0.8 |
| Copper | | |
| Unoxidized | 0.03 - 0.2 | 0.06 - 0.2 |
| Lightly oxidized | 0.4 - 0.5 | 0.4 - 0.5 |
| Heavily oxidized | 0.8 | 0.8 |
| Iron | | |
| Unoxidized | 0.05 - 0.25 | 0.35 |
| Lightly oxidized | 0.35 - 0.5 | 0.45 - 0.5 |
| Heavily oxidized | 0.7 - 0.95 | 0.8 - 0.95 |
| Stainless Steel | | |
| Unoxidized | 0.3 - 0.5 | 0.3 - 0.45 |
| Lightly oxidized | 0.5 - 0.7 | 0.5 - 0.7 |
| Heavily oxidized | 0.8 - 0.9 | 0.8 - 0.9 |
| Gold | | |
| Unoxidized | 0.02 - 0.05 | 0.04 - 0.15 |
| Heavily tarnished | 0.3 - 0.45 | 0.6 - 0.8 |
| Silver | | |
| Unoxidized | 0.01 - 0.03 | 0.02 - 0.05 |
| Lightly oxidized | 0.02 - 0.04 | 0.04 - 0.08 |
| Tin | | |
| Unoxidized | 0.05 - 0.1 | 0.2 - 0.3 |
| Lightly oxidized | 0.25 - 0.3 | 0.25 - 0.45 |
| Heavily oxidized | 0.6 | 0.6 |

Table 1. Representative Emittance of Some Common Materials

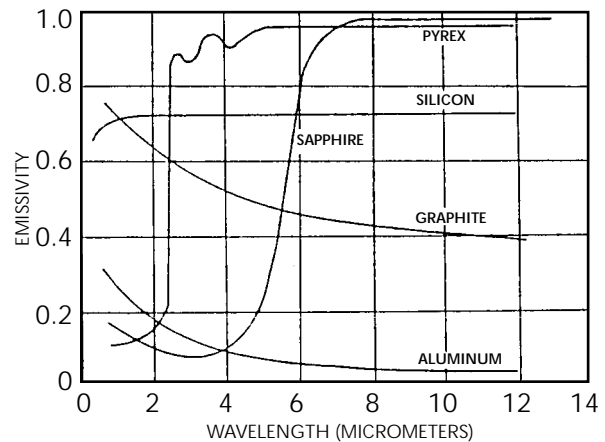


Fig. 5 Spectral Emittance of Some Typical Materials

Table 1 presents ranges of both total and spectral emittance of some common materials. The value of total emittances, of course, is somewhat temperature-dependent. The ranges given are for temperatures likely to be encountered in heat treating or manufacturing operations.

For each surface condition a range of values is given for both total and spectral emittance. The lower values are for polished material. The higher values are for rough-machined material. As materials oxidize, both the total and spectral emittances tend to increase, and the surface condition dependence of the emittance tends to decrease.

The emittance given is for materials in the open. Materials which are enclosed, as in an oven or furnace, have higher apparent emissivities due to

energy reflected from the surroundings. Thus, oxidized steel which has a spectral emissivity of around 0.8 in the open, may have an apparent emissivity of around 0.9 inside a furnace.

THE RESPONSE OF INFRARED THERMOMETERS TO RADIATION

In simplest terms an IRT consists of an optical system and a detector. Both will be discussed in more detail. The output of the detector may be different at different wavelengths. The transmission of the optical elements will depend on wavelength. The output of the detector at any wavelength, therefore, is proportional to the amount radiated by the target, the amount absorbed by the optical system, and the response of the detector at that wavelength.

The calibration function of the thermometer, i.e., how the thermometer output varies with temperature, is the sum of the outputs at all wavelengths at each temperature.

This can be written, using Wien's Law, as:

$$V(T) = KC_1 \int_{\lambda_1}^{\lambda_2} \lambda^{-5} \epsilon^{-C_2/\lambda T} d\lambda$$

Any thermometer can be characterized by an effective wavelength which is the wavelength such that:

$$\lambda_e^{-5} \epsilon^{-C_2/\lambda_e T} = KC_1 \int_{\lambda_1}^{\lambda_2} \lambda^{-5} \epsilon^{-C_2/\lambda T} d\lambda$$

The effective wavelength changes with temperature, but one can calculate the effective wavelength for the calibration function of a thermometer that is applicable between any two desired temperatures, i.e. the measuring range of the thermometer.

THE N FACTOR

At a single temperature or over a narrow range of temperatures, the calibration function can be approximated in the form:

$$V(T) = KT^N$$

A pyrometer receiving radiation from a high temperature target in a wide band of wavelengths would have a calibration function approximately the form of the Stefan-Boltzmann Law, i.e., N would be near 4.

For pyrometers with restricted wavelength response, the value of N is higher.

If $V(T) = KT^N$, the pyrometer may be described as obeying the Nth power law.

It can be shown also that, approximately,

$$N = \frac{C_2}{\lambda_e T} = \frac{14388}{\lambda_e T}$$

where:

λ_e = Effective wavelength in μm .

T = Target temperature, Kelvins

The significance of the N value of an IRT is that it allows a quick estimate of the effect of changing target emittance on the thermometer output when the target temperature is held constant.

If the target is at temperature T and the emittance is ϵ , the output is:

$$V(T) = \epsilon KT^N$$

where K is a constant that depends on the construction of the thermometer.

The output of the thermometer is directly proportional to the emittance. If emittance changes by 10% but the temperature remains constant, the output changes by 10%. However, the output of the thermometer is interpreted in terms of temperature. How is the indicated temperature affected by a change in emittance?

If the calibration equation of the thermometer is written as:

$$V = KT^N$$

then $T = K_1 V^{1/N}$, where $K_1 = K^{1/N}$

For a change in thermometer output, ΔV , the equivalent change in temperature is:

$$\Delta T = \frac{K_1}{N} V^{(1/N - 1)} \Delta V$$

so,

$$\frac{\Delta T}{T} = \frac{K_1 V^{(1/N - 1)}}{NK_1 V^{1/N}} \Delta V = \frac{1}{N} \frac{\Delta V}{V}$$

Therefore, if the output of the thermometer changes by 20%, the indicated absolute temperature will change by $20\%/N$.

Since V is proportional to ϵ , the higher the value of N, the less dependent is the temperature reading on the target emittance.

Remembering that:

$$N = \frac{C_2}{\lambda_e T}$$

it can be seen that, other things being equal, a thermometer with the shortest possible equivalent wavelength should be chosen in order to get the highest value of N and the least dependence on target emittance changes.

The benefit of a high value of N extends to the effects of any variable that changes the output V. Thus, a dirty optical system or absorption by particles, gases, or vapors in the sight path has less effect on indicated temperature if N has a high value.

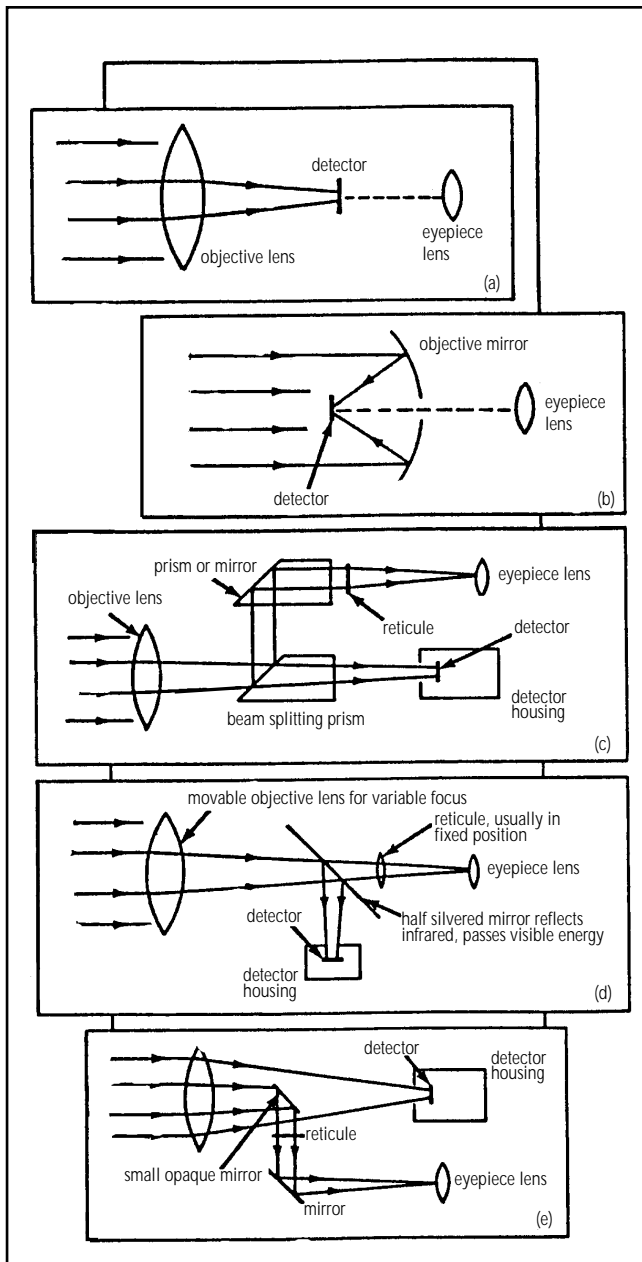


Fig. 6 Common Optical Systems

COMMON INFRARED THERMOMETER CONSTRUCTIONS

Fig. 6 illustrates the most common types of construction found in industrial IRTs. The constructions in (a) and (b) are typical of instruments using detectors, such as thermopiles and silicon cells that give a stable DC millivolt output without pre-amplification.

The arrangement of (a) has also been used for detectors whose DC drift demands that they be used in an AC mode. A spinning disk or vibrating reed interposed between the objective lens and detector, cyclically interrupts the radiation so that the detector sees pulses of radiation. The output signal of the detector is AC. The detector package must be small enough, of course, so that it does not interfere with optical sighting of the target.

If the detector package is too large to permit sighting around it, the arrangements of (c), (d), or (e) are useful. Fig. 7 illustrates a design of the type shown in Fig. 6(e). Optical chopping between the objective lens and the detector is common in these constructions. The back surface of the chopping disc or blade may serve as a local ambient temperature reference. The detector alternately sees the target and the modulating device, which is at local ambient temperature.

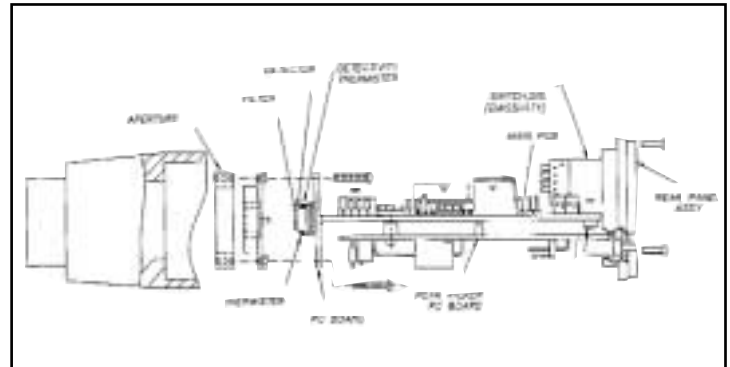


Fig. 7 The Arrangement of One Type of Industrial Infrared Thermometer

In some thermometers a local hot source, a tungsten strip lamp, or other hot surface may be maintained at a known reference temperature. The detector alternately sees the target and the reference source. The resulting AC signal can then be calibrated in terms of the unknown target temperature.

In some ratio thermometers the filters that define the pass band of the two radiation signals that are ratioed may be on the chopping disc.

SURFACE TEMPERATURE INFRARED THERMOMETERS

We have seen that a radiation source with characteristics close to that of a blackbody could be constructed by assuring multiple reflections within a cavity. Fig. 8 illustrates a device for measuring the temperature of the surface of an object based on this principle.

Radiation from the target is multiply reflected from the hemispherical mirror. A detector

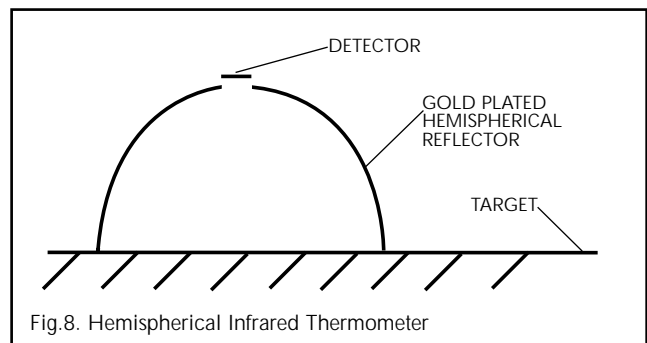


Fig.8. Hemispherical Infrared Thermometer

receives radiation through a small opening in the reflector. The radiation multiply reflected between the mirror and the target appears to the detector to be from a blackbody. A commercial thermometer using this principle can read the temperature of targets with emittance as low as 0.6 without correction. The reflector must be placed close to the surface being measured to exclude extraneous radiation and prevent radiation losses.

ELEMENTS OF INFRARED THERMOMETERS

The selection of a detector and optical elements for an IRT is normally the concern of the thermometer vendor who balances out the conflicting elements of cost, accuracy, speed of response, and usable temperature range. The user should be aware of how the selection of detectors and optical elements influences the range of wavelengths over which a thermometer responds. When applying an IRT to the measurement of products in the presence of atmospheric absorption or reflections from other objects, or when trying to measure the temperature of materials such as glass or plastics, the spectral response of an IRT will determine whether a usable temperature measurement is possible.

DETECTORS

Detectors for IRTs are of three types: thermal, photon, and pyroelectric. Thermal detectors reach an equilibrium temperature proportional to the temperature of the target. The detector output is then interpreted as target temperature. The most common thermal detectors today are thermopiles and thermistor bolometers.

A thermopile consists of one or more minute thermocouples connected in series. The output, as from any thermocouple, is a DC millivoltage. Thermopiles may be manufactured from thin strips of metal or, more commonly, vacuum deposited on a substrate. Usually, both thermopiles and bolometers are blackened with carbon black or other broadband absorbing material so that they respond to radiation throughout the entire spectrum, thus the common term, broadband detectors.

Photon detectors respond to incident radiation by releasing electric charges. In lead sulfide and lead selenide photoconductive detec-

tors, this release of charge is measured as a change in resistance. In photovoltaic detectors, such as silicon, germanium, and indium antimonide, the release of a charge produces a voltage output.

The release of electrons and "holes" in photoconductive and photovoltaic detectors requires that arriving photons have a minimum energy that depends on the molecular structure of the detector material. Thus, all photon detectors have a maximum wavelength (minimum photon energy) beyond which they do not respond. The peak response is usually at a wavelength a little shorter than the cutoff wavelength.

The approximate peak response wavelengths of some photon detectors are:

| Material | Wavelength, μm |
|-------------------|---------------------------|
| Silicon | 0.9 |
| Germanium | 1.7 |
| Lead sulfide | 2.5 |
| Indium arsenide | 3.0 |
| Indium antimonide | 6.0 |

Pyroelectric detectors respond to changes in received radiation with a changing surface charge. Because it responds to changes in incoming radiation, the detector need not reach thermal equilibrium when the target temperature changes. However, the incoming radiation must be chopped, and the detector signal cannot be utilized directly. The detector changes can be likened to a change in charge of a capacitor, which must be read with high impedance circuitry.

Pyroelectric detectors bear a radiation-absorbent coating, so they can have a spectral response as broad as thermal detectors, or, by selecting the characteristics of the coating, a more restricted response.

OPTICAL SYSTEMS

The optical system of an IRT may be composed of lenses or mirrors or combinations of both. In general, the reflectivity of mirrors is not significantly dependent on wavelength over the range of wavelengths used for industrial temperature

| Material | Refractive Index | Cut-off Wavelength - μm | Mechanical & Chemical Stability | Remarks |
|--------------------|------------------|------------------------------------|---------------------------------|--|
| Glass | 1.5 | 2.8 | Excellent | Excellent transmission in the visible. |
| Fused Silica | 1.4 | 4.0 | Excellent | Excellent transmission in the visible. |
| Calcium Fluoride | 1.4 | 10.0 | Good | Good visible transmission. Relatively high chromatic aberration. |
| Arsenic trisulfide | 2.35 | 12.0 | Good | Low transmission in the visible. Low chromatic aberration. |
| Zinc Sulfide | 2.25 | 14.0 | Good | Very low transmission in the visible. |
| Polyethylene | — | 20.0 | Poor | Sometimes used as window. Easily distorted or crazed by heat |

Table 3. Properties of Lens and Window Materials

measurement. Therefore, mirror systems do not determine the spectral response of the pyrometer. A mirror system must usually be protected from dirt and physical damage by a window. The characteristics of the window, and those of the detector, determine the band of wavelengths over which the thermometer responds.

Mirror systems have been common mainly in fixed focus optical systems. To vary the focus of an optical system requires that at least one element be movable. Providing for this motion in mirror systems is often more complicated than in lens systems. The selection of lens and window materials is always a compromise between the optical and physical properties of the material and the desired wavelength response of the pyrometer. The properties of some typical lens and window materials are given in Table 3.

FIELD OF VIEW

The field of view (FOV) of an IRT is a statement of the size of the target at a specified distance from the thermometer. This may be stated in the form of a diagram, a table of target sizes versus distance, sometimes simply as the target size at the focal plane and the distance to the focal plane, or as an angular FOV.

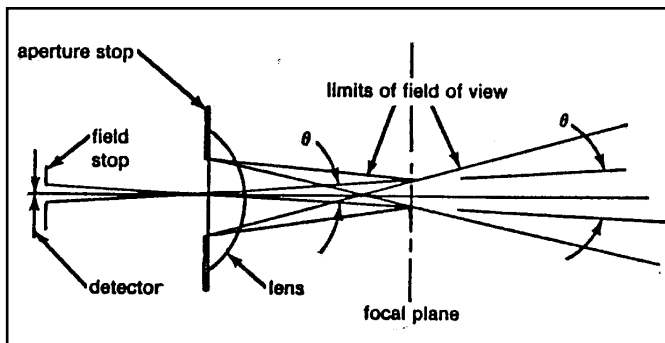


Fig. 9 The Field of View of a Perfect Infrared Thermometer

If the output of an IRT is to be the same as its calibrated output, the target must fill the FOV. If the target fills the FOV at any distance from the thermometer, the output will be the calibrated output, or nearly so, as discussed below. The image of the field stop in the focal plane in most thermometers is larger than the diameter of the field stop. θ is the angular FOV. Between the aperture stop and the focal plane, the FOV is determined by the stop diameter and the image diameter.

Lines drawn from the extremities of the image to the extremities of the aperture stop enclose the FOV. Beyond the focal plane the field of view is determined by rays extending from the extremities of the aperture stop through the extremities of the image in the focal plane. Fig. 9 shows that

only if the image in the focal plane is large relative to the lens, and the focal plane is many lens diameters from the lens, will the actual field of view be given by the angle θ . The actual FOV is always larger.

Most thermometers have images in the focal plane that are the same diameter as the lens or smaller, so the statement of an angular FOV is not sufficient definition. Therefore, diagrams or tables are usually used to define the FOV. In practice, any statement of the FOV is only an approximation because of spherical and chromatic aberration in the optics. Spherical aberration is caused by the fact that rays hitting the lens remote from its axis are bent more than rays passing the lens near its axis. A circular field stop is therefore imaged as a circle with a fuzzy halo around it. Mirrors also have spherical aberration.

Chromatic aberration occurs because the refractive index of optical materials changes with wavelength. At shorter wavelengths the refractive index is lower, and rays exiting are bent more and focus nearer the lens. Rays of longer wavelengths are focused farther from the lens. The image of a field stop over a band of wavelengths is therefore a fuzzy image.

Other and generally smaller contributions to fuzziness of the FOV are scattering of rays of light by imperfections in the optical material and reflections from the internal parts of the IRT. Good quality materials minimize the former cause. Roughening and blackening of interior surfaces to reduce reflections reduce the latter effect.

There are no standards at present for stating the FOV of IRTs. Some manufacturers state an FOV that includes the effects of aberrations; others do not. In practice, it is preferable to select an FOV which is smaller in diameter than the target, but if the target and the FOV diameters are almost the same size, it may be advisable to determine the FOV experimentally as follows:

Sight the IRT on a target that gives a steady, uniform source of radiation. At the focal plane, interpose a series of apertures of different diameter between the IRT and the target, and plot the output of the IRT against the aperture area. For aperture areas less than the nominal target area, the output of the IRT should increase directly proportional to aperture area. Above the nominal target area the output should increase only a small amount with further increases in aperture area.

A perfect IRT would show no increase, but no such IRT exists. Increases of a few tenths of a percent in output for each doubling of the aperture area indicate that the nominal field of view takes into account the effects of aberrations. If these are not taken into account, the IRT may show a significant increase in output as the viewable target area is increased above the nominal value.

SIGNAL CONDITIONING

LINEARIZATION

The calibration curves of detector output versus temperature of all detectors is nonlinear because, as was explained in a previous section, the equations relating the amount of radiation emitted by an object are inherently power functions. If the output of a detector is approximated by $e = KT^N$, N has a value of at least 4, and it can be as high as 20. Inexpensive microprocessors now permit such signals to be linearized easily, and most IRTs provide a linear output as a standard feature. An exception is found when extreme accuracy is required. In such cases the linearizing function is sacrificed in order to avoid the small errors in most linearizers.

SAMPLE AND HOLD

The sample and hold function is useful where it is desired to measure a product temperature whenever a selected event triggers the measurement. The thermometer measures temperature at that instant, disregarding earlier or later measurements. Analog sample and hold circuits always exhibited a slow drift of the measurement during the "hold" period, but modern digital instrumentation can hold the value without degradation for an indefinite time.

PEAK AND VALLEY PICKING

In some applications the temperature of interest is the highest temperature within the FOV during a given period. This might be true of a target that is occasionally obscured by smoke or cannot be viewed continuously (as in a series of objects, such as bottles on a conveyor). The electronics interface then can be programmed to "remember" the highest temperature it saw in the sampling period (see Figure 10).

Valley picking is the inverse of peak picking, useful where the lowest temperature measured is the preferred value for control.

AVERAGING

Averaging is usually used to eliminate rapid excursions of the temperature reading from the norm, where such excursions would cause difficulty in interpreting the record, or cause upsets in a control system. Such conditions could be encountered in the measurement of metal surfaces which are partially covered in scale. A common way to average is to slow the response of the electronics with an RC filter, but the equivalent function is often performed by the software in microprocessor-based signal conditioners.

SIGNAL MODIFYING ALGORITHM

Many difficult measurement problems can be solved by the correct selection of wavelength, optics and conventional signal conditioning, but there is a residue of such problems that will not yield to this approach. In some such cases, providing that sufficient data has been accumulated about the characteristics of the process, the signal measured by the IRT can be manipulated by software generated algorithms, developed from the process data. An example of such an application is the measurement of aluminum temperature, where the emissivity is very low, changes rapidly with time, and differs from alloy to alloy.

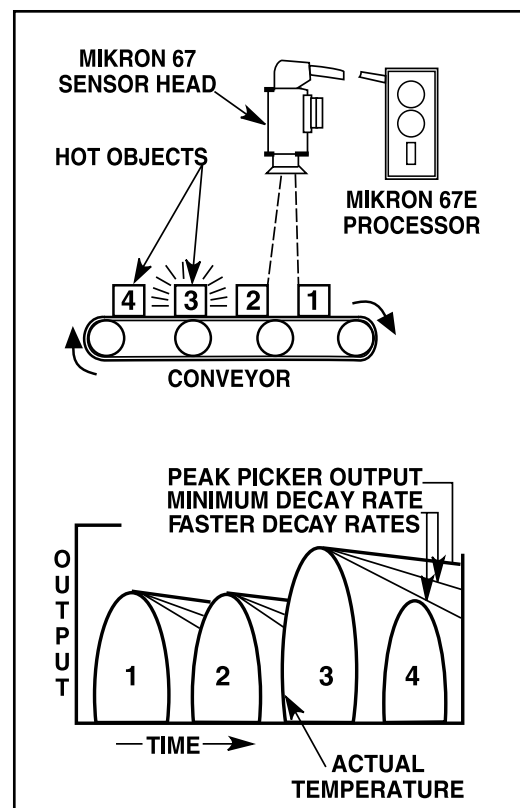


Fig. 10 Output trace for a typical conveyor system showing peaked outputs.

BLACKBODY CALIBRATION SOURCES FUNCTION AS STANDARDS

As recently as the late 1970's, virtually no one outside organizations such as national standards laboratories, some large industrial corporations, and manufacturers of infrared temperature sensors knew what a blackbody calibration source was. Most of the users, and even some of the manufacturers of the device, had only a rudimentary understanding of this important calibration standard. This lack of knowledge quite often led to the purchase or construction of unsatisfactory sources. This, in turn, contributed significantly to a mistrust of infrared temperature-sensing accuracy and limited use of related techniques.

With the increasing use of more-sophisticated infrared-sensing techniques such as thermography and the proliferation of infrared-sensing applications in meteorology, earth monitoring by satellite, spectrographic analysis, weaponry, and security surveillance, the blackbody calibration source, while not quite commonplace, is now better understood. It can be found as frequently on the factory floor and the missile-testing range as in the laboratory.

For those who are unfamiliar with the blackbody calibration source—once referred to as a blackbody furnace—because early infrared temperature sensors could only measure elevated temperatures—this device is the best real-life approximation of a target surface that is a theoretically perfect emitter of infrared energy. In other words, it is a surface that reradiates 100% of the infrared energy it receives and does not reflect or transmit any of the received energy.

In the real world, however, only the interior surface of a totally enclosed cavity that is opaque to infrared energy will exhibit perfect emission. Because the blackbody calibration source is mainly used for the calibration of electro-optic measuring devices, it is implicit that the measuring device must be able to "see" into the sphere, and this factor rules out a totally enclosed cavity (see photo).

The objective of a blackbody calibration source design, therefore, is to provide an accessible target surface of known emissivity, known temperature, and prescribed spectral-radiation characteristics. The best design compromise is a sphere with the smallest practical aperture, preferably with a tube extension from the aperture (see Fig. 1) A carefully constructed source of this type will produce a uniform surface with an emissivity of 0.999, or, in other words, it is a 99.9% efficient emitter. The 0.001 deficiency is attributable to the aperture, because this degrades the total internal reflection required for a theoretically perfect blackbody emitter.



Operator calibrates a transfer standard (lower foreground) – an infrared thermometer with 0.1°C resolution – with a blackbody calibration source that provides temperatures from 600° to 3000°C.

Practical day-to-day applications of blackbody calibration sources impose severe demands on the spherical design. In medium- to high-temperature sources, the sphere is generally molded from refractory material with resistance-heating elements bonded to the outer surface. This form of construction results in vulnerability to damage from mechanical shock or from thermal shock due to rapid changes in temperature. Also, because the ratio of aperture diameter to sphere diameter significantly influences the source emissivity, a large-diameter (25 to 50 mm) aperture requires a commensurately large sphere, typically 200 to 300 mm in diameter. This results in an overall assembly that is too large for easy transportation or to be accommodated in a crowded laboratory.

These operational demands have inspired a variety of alternative configurations to meet such needs as portability, small size, ruggedness, rapid and frequent source temperature change, and wide temperature range capability. (see Fig. 2) These cavity design alternatives to the sphere are capable of producing source emissivities of 0.98 to 0.99, over temperature ranges from -10°C to 1700°C.

A good design is exemplified by a source that has an adequate aperture diameter for its intended use, adjustable temperature over the desired working range, uniform temperature distribution

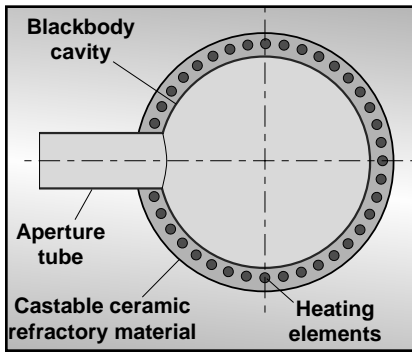


FIGURE 1. To calibrate infrared-energy-measurement instruments such as detectors, a spherical blackbody calibration source makes the best design compromise; it includes the smallest possible practical aperture, preferably with a tube extension.

over the target surface, accurate temperature control, fast stabilization at a new temperature setting, long-term temperature stability, and, of course, the highest emissivity over the prescribed spectral band. Other considerations that may enter into the design are aperture acceptance angle, overall size, portability, power consumption, and the need for remote control and data acquisition.

CALIBRATION TRACEABILITY

The most common application for blackbody sources is the calibration of radiometers and infrared thermometers. Because these devices are emissivity dependent—that is, their measurement accuracy is related to the infrared emitting property of the target of interest—the only way to determine measurement uncertainty with a high level of assurance is to calibrate against a source of known emissivity and temperature. This then raises the question of how to be assured that the calibration source is accurate, and superficially this would seem to lead into a realm of doubt that has no end, other than in crippling paranoia. Fortunately, the Calibration Traceability protocol saves the intending user from this fate.

Calibration traceability is based on a hierarchy of calibration standards, with the national standard at the top of the accountability tree. National standards organizations such as the National Institute of Standards and Technology (NIST) in the USA and the National Physical Laboratories in the United Kingdom possess three primary types of radiometric calibration sources; fixed-temperature, freezing-point blackbody sources; variable-temperature blackbody sources; and tungsten-strip lamp sources.

More important in terms of their status as custodians of primary temperature standards, national standards organizations are able to use radiometric measurement instruments that are capable of higher accuracy than could be practicably achieved for working instruments in the field. This is due partly to the design and partly to being able to operate them in a closely controlled environment. In hierarchical terms, NIST's standards are referred to as "Primary Standards." All other calibration standards are referred to as

either "Transfer" or "Working Standards."

In the classical sense, the calibration-traceability hierarchy is intended to operate with the user of infrared temperature-measuring instruments periodically submitting transfer standards to the national standards organization for calibration against a primary standard. The transfer standard may be a resistance thermometer, thermocouple, infrared thermometer, or variable-temperature blackbody source. Once the measurement uncertainty of the transfer standard has been established and documented, it is used as a comparator for checking other transfer standards or for checking working standards. Its calibration integrity is maintained by special manufacturing methods and careful storage and use. The reality of this classic calibration traceability protocol is that the time needed and the cost involved for national standards organizations to carry out this work usually is prohibitive for most intending participants, due to the standards organizations'

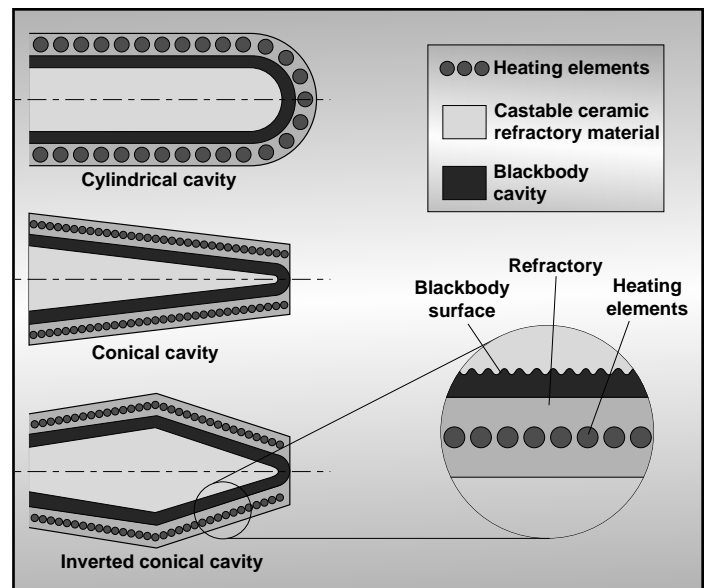


FIGURE 2. To address needs such as portability, small size, ruggedness, rapid and frequent source temperature change, and wide temperature range capabilities, blackbody calibration standards incorporate nonspherical cavity configurations.

limited physical resources and budgets.

TOOLS FOR CALIBRATION STANDARDS

The increasing demand for calibration traceability brought on by a high-technology environment and the pervasiveness of quality-assurance programs in manufacturing has coincided with the commercial development of freezing-point blackbody calibration sources, high-performance variable-temperature blackbody calibration sources, and tungsten-strip lamp systems. These devices have enabled private-sector organizations to provide calibration assurance to a level that is close enough to national standards for most users and more than adequate for quality-assurance

programs such as ISO 9000. Private-sector calibration laboratories usually cater to in-house needs, but some of these laboratories also offer the service commercially to outside customers.

The assurance that the commercial calibration laboratories can offer the user of radiometric sensors is derived largely from the freezing-point blackbody calibration sources. These sources provide fixed-point, primary calibration standards for the checking of transfer standards at discrete temperatures from 29.76°C to 1084.62°C.

The freezing-point calibration source principle of operation is based on the temperature arrest phenomenon, which occurs when a molten substance changes to a solid. During the cooling curve arrest period, the substance remains at a predictable temperature for several minutes and then continues to cool. In the case of high-purity metallic elements, the predictability of the arrest temperature is very precise and thus can be used as a primary temperature calibration standard.

For example, the Mikron M380 Series of Freezing Point Sources is produced in eight bench-top sized models, each dedicated to the freezing point of a particular metal, such as copper, gold, silver, aluminum, zinc, tin, indium, or gallium. Computer software is available that, in conjunction with a Mikron M190 infrared thermometer transfer standard, facilitates clear and unambiguous determination of the freezing point and lends itself to automation or use by semi-skilled operators.

For higher-temperature calibration, especially for infrared sensors, a modern version of the accepted standard calibration method using a tungsten-strip lamp is available. This instrument will also calibrate older sensors of the disappearing-filament type. In these, the sensor's heated and calibrated filament is superimposed on the image of the target object. Filament temperature is adjusted until the filament seems to disappear against the target. At this setting, filament and target are the same temperature. Then the actual temperature is determined from the sensor's calibrated filament setting.

One version is a bench-top source covering the range of 800°C to 2300°C in one-degree steps. It has a programmed controller to eliminate refer-

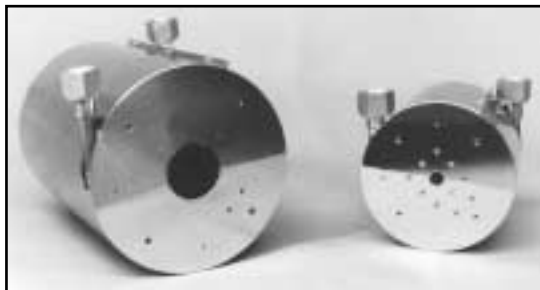


FIGURE 3. When designed with forced cooling to dissipate the heat generated, a blackbody calibration source can be operated in a vacuum to simulate conditions in space. (It will also operate in air.)

ence tables for lamp current versus temperature. The source has a current limiter to control the rate of lamp current change and thereby extend lamp life. Now, more-easily used higher-emissivity carbon-tube sources are available, which may displace the tungsten-strip lamp as a calibration method.

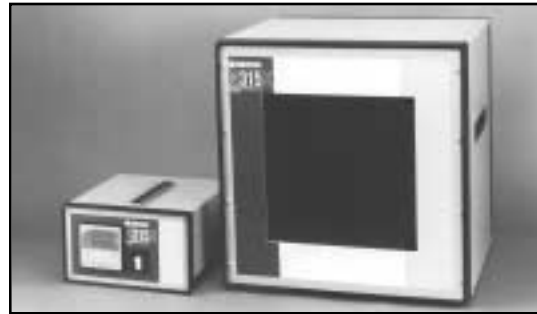


FIGURE 4. For calibrating thermal imaging systems or mapping and surveillance equipment, or for long-path spectrophotometers, a calibration source requires a large target area. Source (on the right) area is 305mm square; the controller is on the left.

APPLICATIONS

While the use of blackbody calibration sources is increasing, more exotic applications for these sources are being developed. Special conditions such as outer space and many modern high-technology production techniques have resulted in calibrator designs that were inconceivable a few years ago.

Compact and portable blackbody calibration sources are available. Blackbody sources now have the capability of operating in air or in vacuum. (see Fig. 3) The vacuum environment presents the special problem of dissipating heat when the source temperature is being reduced.

Calibration of thermal imaging systems and spectrographic analyzers requires a source with a very large target area. (see Fig. 4). Such sources are used for the calibration of thermal-imaging systems and spectrographic analyzers.

The calibrator shown in use in p. 1 is capable of providing extremely high source temperatures, up to 3000°C. The closed-end graphite-tube target must be purged with nitrogen or argon gas to prolong its life. Even with purging, target life is typically several hours at between 2600°C and 3000°C, but it will last for many months at lower temperatures. (The design allows for rapid replacement of the target.) Temperature set point is adjustable remotely via an RS422 port. A PID controller regulates target temperature precisely.

Proper calibration standards must be used to ensure accurate performance of many electro-optical systems, especially infrared detectors and imaging arrays. More diverse application requirements will likely be developed to test the ingenuity of design engineers. And, as in other fields of technological endeavor, the spin-off will contribute to the advancement of more-conventional calibration standards.

FREEZING POINT BLACKBODY RADIATION SOURCES FOR THE TEMPERATURE RANGE 29.78° TO 1084.62°C

Freezing points of In, Sn, Zn, Al, Ag, Au and Cu, along with the melting point of Ga, are among the defining fixed points of the International Temperature Scale of 1990 (ITS-90). Accordingly, blackbody sources have been commercially produced that utilize the freezing/melting points of the above metals for precision radiometric calibrations of non-contact thermometers. The cavity emissivity is estimated to be 0.999 and the fixed point metals have a nominal purity of 99.9999%. In the following paper, we analyze the freezing plateau of a Gold FPBB and show that the accuracy of calibrating a Narrow Band Radiometer (NBR) at 960nm is $(-0.17 \pm 0.02)\text{K}$.

INTRODUCTION

Non-contact thermometry is playing an increasingly important role in industrial applications where contact type thermometers cannot be employed. These applications include semiconductor crystal growing, glass processes, aluminum rolling and extrusion and temperature measurements in the steel reheat furnaces.¹ The accuracy and precision required by these industries has provided impetus for Mikron, as a manufacturer of non-contact thermometers as well as blackbody calibration sources, to develop more accurate and precise radiometers as well as blackbody calibration sources. Consequently, a series of freezing point blackbody (FPBB) sources have been developed, covering the range from 29.76 to 1084.62°C, using the freezing points of In, Sn, Zn, Al, Ag, Au and Cu, along with the melting point of Ga. The normal freezing/melting points of these metals are defined by the International Temperature Scale of 1990 (ITS-90).²

Each FPBB source, therefore, is a primary calibration standard whose radiance temperature is transferred to secondary, variable temperature blackbody sources. The apparent emissivity of these secondary sources, as determined by two color measurements, is estimated to be in excess of 0.99.

The following paper presents a thorough analysis of a Gold FPBB source. There is no attempt to measure the thermodynamic temperature of the Au point and we use the value 1337.33K as established by the ITS-90. The measurements then deal with deviations from this temperature. The goal of the paper is to address the question: What is the magnitude of the uncertainty in the calibration of a radiometer due to the uncertainty of the FPBB source? The paper is organized as follows. The basic construction of the blackbody is reviewed first. Next, the experimental configuration for the

measurement of the freezing plateau of Gold is presented, and in the following section, the experimental results and analysis are given. It is estimated that the total accuracy in calibrating a narrow band radiometer at 960nm using this source is $(-0.17 \pm 0.02)\text{K}$. Finally, the paper concludes with a brief summary of the results and their implications on practical radiometric sensor calibration.

DESIGN OF THE BLACKBODY SOURCES

The basic construction of a freezing point blackbody (FPBB) source is shown below in Figure 1. The scheme embodies some aspects of earlier works in FPBB design.^{3,4} It should be noted that this drawing is not to scale and its intention is merely to serve as a generic layout of the FPBB sources. The high purity metal is placed inside the graphite crucible. A cylindro-conical graphite cavity is placed within the crucible such that the molten metal completely surrounds the walls of the cavity. The crucible is heated by the heating elements. A calibrated thermocouple measures the crucible temperature and thus serves as the source of the feedback signal for the proportional integral derivative (PID) controller. The temperature of the furnace can therefore be set at the desired value above or below the freezing point, and the automatic temperature controller will maintain the temperature at the desired value.

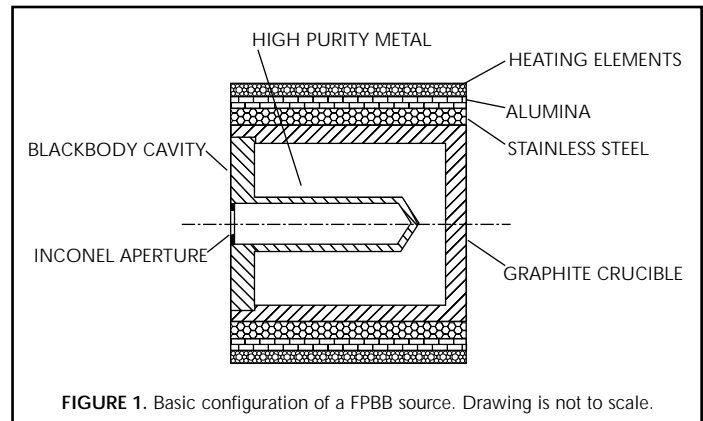


FIGURE 1. Basic configuration of a FPBB source. Drawing is not to scale.

For the high temperature sources (Cu, Au and Al) the crucible is maintained in an inert Argon atmosphere to prevent oxidation of the graphite. An Inconel aperture is placed at the mouth of the cavity, thus providing a "lid" for the cylindro-conical graphite cavity. Each FPBB source is packaged in a compact, bench top mounting enclosure which includes the controller. The total mass of the unit is less than 10Kg. For the

realization of the Gold freezing point, 1337.33K, the metal is first completely melted by setting the controller temperature approximately 20K above the freezing temperature at 1357K. To insure that the metal is completely molten, the furnace is kept at this temperature for approximately 30 minutes. Then the temperature controller is set to 1327K, ~10K below the freezing point. The temperature of the freezing metal is then recorded as a function of time by using a 960nm narrow band radiometer as described in the next section.

EXPERIMENTAL ARRANGEMENT

A schematic depicting the radiometer is shown below in Figure 2. An achromat objective lens, O, 30mm in diameter with an effective focal length of 124.3mm is positioned at the front end of the radiometer. The achromat is optimized for the wavelength region 0.70 μ m to 1.1 μ m. A 21.2mm "constant energy" aperture, A1, is positioned behind the objective lens in order to ensure that the amount of energy collected does not change when the distance from the objective to an infinitely large target is altered. The separation between the back side of the objective lens and A1 can be adjusted, from 25.4mm to 50.8mm, to allow for varying target distances. A small mirror (not shown) positioned in the path of the gathered light directs a small portion of the light to an eye piece, thus providing visual focusing at the target.

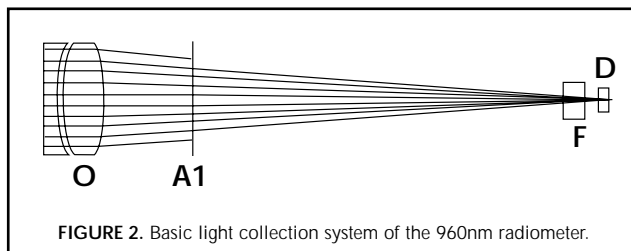


FIGURE 2. Basic light collection system of the 960nm radiometer.

The undeviated light proceeds toward a 960nm, 11nm FWHM, interference filter, F. The distance from the back side of the objective lens to the filter varies according to the target distance from ~130mm to ~155mm. After passing through the filter, the light proceeds ~8mm to a 0.79mm aperture that is placed approximately 1mm in front of the active area of a 1mm diameter Silicon photodiode, D. The silicon photodiode is operated in the photovoltaic mode. The current from the photodiode is measured by a Keithley 485 precision picoammeter and is then inputted in the form of a voltage to a Fluke 8842A voltmeter. The Fluke meter has a precision of 5 digits in the voltage range of interest. This results in a resolution of approximately 5.6mK near the Gold freezing point. The output of the Fluke is then sent to a computerized data acquisition system.

The field of view (FOV) of the radiometer is defined as the target distance to diameter ratio

when the target diameter is such that the energy collected is equal to 98% of the energy that would be collected for an infinitely large target. In this way the FOV is experimentally determined to be ~140:1. In the experiments reported in this paper the target distance is approximately 50cm and therefore the target size is 3.6mm. Since the target size is about 40% smaller than the cavity aperture, 6mm, negligible errors in temperature determination due to radiation originating from outside the cavity aperture are expected.

EXPERIMENTAL RESULTS

The freezing curve of a Gold freezing point black-body (FPBB) source is measured three times using the radiometer described in the previous section. The three curves are then averaged and the resultant average freezing curve is used for data analysis. A typical freezing curve is shown below in Figure 3. The metal supercools by approximately 0.5K below the equilibrium freezing temperature. The supercool marks the onset of nucleation at the cavity walls. The solid continues to grow into the melt until all of the liquid is solidified. At this point in time the freezing plateau begins to slope downward. For computational purposes only the steady state region from t=4min to t=9min is used in this analysis. Using Wien's approximation to Planck's law, we calculate the variation in the measured temperature about the equilibrium freezing point of Gold:

$$\delta T = \frac{\lambda T^2}{14388} \ln\left(\frac{\Phi}{\Phi_0}\right) \quad (1)$$

where $T = 1337.33\text{K}$, $\lambda = 0.960\mu\text{m}$, Φ is the average flux and Φ_0 is the flux. The 3σ temperature variation about the average temperature is thus calculated to be $\pm 0.023\text{K}$.

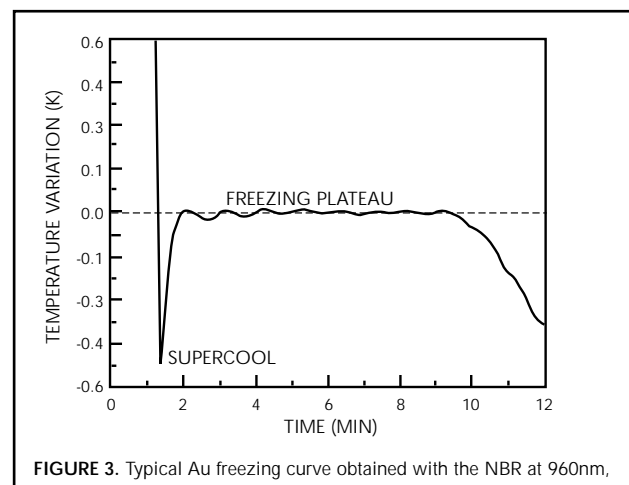


FIGURE 3. Typical Au freezing curve obtained with the NBR at 960nm.

The purity of the freezing metal is of extreme importance in fixed point thermometry. The addition of small amounts of impurity atoms to an otherwise pure substance alters the freezing point of

the pure substance.^{5,6} Depending upon the ratio of the solid solubility of the impurity to its liquid solubility, the equilibrium freezing point of a substance is either elevated or depressed. This change in the freezing point will manifest itself through a sloping freezing plateau.⁷ In other words, the formation of the first solid after nucleation will occur at a temperature different from the temperature at which the last solid is formed. It should be cautioned, however, that a sloping plateau may also be due to the spatial variations in the distribution of the emitted radiation at different times during the freeze and the melt.⁸ In the experiments on Gold, there is no evidence of a slope on the steady state freezing plateau. It must be kept in mind, however, that since the resolution is limited to 5.6mK the effect of impurities on the Gold freezing point cannot be ruled out. The freezing point change due to the impurity content must therefore be considered. As a first attempt at estimating the change in the freezing point, the slope of the binary alloy phase diagrams in the vicinity of the zero impurity concentration is used.⁹ However, this analysis is not possible in the case of phase diagrams in which the equilibrium solidus curve has a very large slope and hence cannot be resolved from the diagram. As a result, the Clausius-Clapeyron equation¹⁰ is examined in determining the freezing point depressions. Comparison between the depressions obtained from the phase diagrams with those obtained from this equation shows that the latter predicts freezing point depressions that are at most half as much as the depressions extrapolated from the phase diagrams. Hence, the Clausius-Clapeyron equation is used in determining the freezing point depressions. The Clausius-Clapeyron equation for an ideal dilute binary solution, assuming negligible solid solubility of the impurity, is given by

$$\Delta T \cong \frac{RT^2}{L_f} \ln(N_A) \quad (2)$$

where ΔT is the freezing point depression, T is the freezing temperature of the pure substance, N_A is the mole fraction of the pure substance, R is the universal gas constant and L_f is the heat of fusion of the pure substance. Given the mass fraction of the impurities, as provided by the manufacturer, the freezing point depression due to each impurity is calculated independently of the others. Adding the contribution from each impurity, a total freezing point depression of 2.4mK is calculated, as detailed in Table 1. The freezing point elevation due to Titanium is estimated from the phase diagrams. By making the conservative assumption that the calculated value is half that of the true value, a worst case freezing point depression of 6mK is estimated. Therefore, the temperature of the solid-liquid interface within the crucible is estimated to be 1337.324K. It is further assumed that the temperature of the solid-liquid interface is the temperature that is immediately in contact with the graphite crucible. In other words,

we are ignoring temperature gradients across the freezing metal.

| Impurity | Mass Fraction (ppm) | Freezing Point Change (mK) |
|----------|---------------------|----------------------------|
| Ag | 0.1 | -0.2 |
| Ca | 0.1 | -0.6 |
| Fe | 0.1 | -0.4 |
| Mg | 0.3 | -2.8 |
| Si | 0.1 | -0.8 |
| Ti | 0.5 | +2.4 |
| | | -2.4mK Total change |

The radiometric method described in this paper, however, relies on the cavity temperature and not on the temperature at the solid-liquid interface within the crucible. Since the graphite walls of the cavity have a finite thickness and a relatively small thermal conductivity, there will be a temperature drop across the wall from the freezing metal to the inside of the cavity. The temperature drop across the cavity walls is estimated by considering the thermal conduction power from the solid-liquid interface to the inside of the graphite cavity and the radiation power loss from the cavity to the environment. The heat transfer rate from the freezing metal across the graphite crucible base is given by

$$q_c = \kappa A \frac{(T_{Au} - T_{cavity})}{\Delta X} \quad (3)$$

where T_{Au} is the temperature of the freezing metal, T_{cavity} is the temperature inside the cavity, A is the area of the crucible base, κ is the thermal conductivity of the graphite at T_{Au} and ΔX is the wall thickness. If the crucible base is not contained within a cavity, and the only loss mechanism for the surface is radiation, then the power inputted from the freezing metal q_c would be radiated by the surface to the ambient. The radiated power q_r is given by

$$q_r = \epsilon_{wall} \sigma A (T_{cavity}^4 - T_{ambient}^4) \quad (4)$$

where ϵ_{wall} is the graphite emissivity and σ is the Stefan-Boltzmann constant. However, if the base is surrounded by a wall (cavity), the radiated power becomes

$$q_r = \frac{(1 - \epsilon_{cavity})}{(1 - \epsilon_{wall})} \epsilon_{wall} \sigma A (T_{cavity}^4 - T_{ambient}^4) \quad (5)$$

where ϵ_{cavity} is the cavity emissivity. Equating Equations 3 and 5, we obtain an approximate solution for the temperature drop across the graphite wall:

$$(T_{Au} - T_{cavity}) = \frac{(1 - \epsilon_{cavity}) \Delta X}{(1 - \epsilon_{wall}) K} \epsilon_{wall} \sigma (T_{cavity}^4 - T_{ambient}^4) \quad (6)$$

It is clear from equation 6 that as the cavity emissivity approaches 1, the temperature drop across the wall approaches zero. An approximate method is used to calculate the apparent emissivity of the graphite cavity¹¹ to be 0.99925, using a graphite emissivity of 0.833 (Ref. 12) and not considering the enhancing effect of the conical end of the cylindrical cavity. However, less than ideal conditions are assumed and the cavity emissivity is estimated to be 0.999. This emissivity is 0.1% better than the apparent emissivity in the absence of the aperture (lid) on the cylindrical cavity. Consequently the estimated cavity emissivity can be confidently assumed to be not higher than the true cavity emissivity. Hence, for calculating the temperature drop across the cavity wall, using equation 6, the worst case conditions are assumed: $\epsilon_{\text{cavity}} = 0.999$, $\epsilon_{\text{wall}} = 0.833$, $\Delta X = 0.27\text{cm}$, $\kappa = (0.54 \pm 0.03)\text{W/cmK}$, and $T_{\text{Au}} = 1337.324\text{K}$. For the ambient temperature 298K is assumed; however, it can readily be observed, from equation 6, that the effect of the ambient temperature on the temperature drop is negligible and for all practical purposes that term may be dropped. Inserting all of the above parameters in equation 6, we obtain $T_{\text{cavity}} = (1337.280 \pm 0.002)\text{K}$. By adding the $\pm 0.023\text{K}$ noise in quadrature to T_{cavity} we obtain $T_{\text{cavity}} = (1337.280 \pm 0.023)\text{K}$.

A radiometer viewing the cavity, however, assumes that the cavity emissivity is 1, and as a result outputs an apparent temperature T_a given by:

$$\frac{1}{T_a} = \frac{1}{T_{\text{cavity}}} - \frac{\lambda}{14388} \ln(\epsilon_{\text{cavity}}) \quad (7)$$

Inserting $T_{\text{cavity}} = (1337.280 \pm 0.023)\text{K}$, $\lambda = 0.960\mu\text{m}$, and $\epsilon_{\text{cavity}} = 0.999$ in equation 7, we obtain $T_a = (1337.1610.023)\text{K}$. Therefore, using the Gold FPBB source, the total accuracy in calibrating a narrow band radiometer at $0.960\mu\text{m}$ is $(-0.17 \pm 0.02)\text{K}$.

CONCLUSION

Using the freezing point blackbody (FPBB) sources, high quality transfer standard radiometers may be calibrated. For example, assuming that the effective wavelength of the transfer standard radiometer does not vary with temperature, one can use any two FPBB sources to obtain the mean-effective wavelength of the radiometer. Then the radiance temperature of any variable temperature blackbody (VTBB) source may be easily determined by dividing the flux from it to the flux from a FPBB source and using Planck's law. Hence, using transfer standard radiometers, radiance temperature is routinely transferred to VTBB sources, which are in turn used for the calibration of non-contact thermometers. In this way a hierarchy of calibration standards has been established that is used in practical radiometric sensor calibration.

It was shown above that using a Au FPBB, a narrow band radiometer (NBR) at 960nm can be calibrated to an accuracy of $(-0.17 \pm 0.02)\text{K}$. It should be noted, however, that this is not the total accuracy that would be obtained in the calibration of a NBR since other factors, such as the linearity of the detector and the size of source effect, would also contribute to the calibration error.¹³ An approximate relation between the calibration error of the NBR and the uncertainty in the temperature of the FPBB sources is given by:

$$\delta T \cong T^2 \left[\frac{\delta T_a}{T_a^2} + \left(\frac{\ln r_m}{\ln r_s} \right) \left(\frac{\delta T_\beta}{T_\beta^2} + \frac{\delta T_a}{T_a^2} \right) \right] \quad (8)$$

where T_a , T_β , δT_a , δT_β are the temperatures and the associated uncertainties of the a and the β FPBB sources, T is the measured temperature, r_m is the ratio of the flux at T to that at T_a and r_s is the ratio of the flux at T_a to that at T_β . It can be noted from equation 8 that the error increases quadratically with temperature and in direct proportion to the errors and the uncertainties associated with the FPBB sources. Consequently, an accurate knowledge of the temperature of the FPBBs is extremely important since they are used for establishing the effective wavelengths of the NBRs as well as serving as pivotal points of calibration.

In both industry and research institutions, increasingly accurate non-contact temperature measurements are demanded. Thus, the uncertainty of these measurements has to be established through an accurate means for calibrating infrared thermometers, radiometers, imaging pyrometers, spectrographic analyzers, and related non-contact instruments. The FPBB source is a useful and compact primary standard for calibrating such instruments, either directly or indirectly through the use of VTBB sources.

References:

1. J. C. Richmond and D. P. DeWitt, eds., *Applications of Radiation Thermometry* (American Society for Testing and Materials, Philadelphia, 1985).
2. H. Preston-Thomas, "The International Temperature Scale of 1990 (ITS-90)," *Metrologia* **27**, 3-10 (1990).
3. F. Sakuma and S. Hattori, "A practical-type fixed point blackbody furnace," in *Temperature, Its Measurement and Control in Science and Industry*, J. F. Schooley, ed. (American Institute of Physics, New York, 1982), Vol. 5 pp. 535-539.
4. J. Fischer and H. J. Jung, "Determination of the thermodynamic temperatures of the freezing points of silver and gold by near-infrared pyrometry," *Metrologia* **26**, 245-252 (1989).
5. M. C. Flemings, *Solidification Processing* (McGraw-Hill, New York, 1974).
6. L. S. Darken and R. W. Gurry, *Physical Chemistry of Metals* (McGraw-Hill, New York, 1953), Chaps. 10-12, pp. 235-325.
7. E. H. McLaren, "The freezing points of high purity metals as precision temperature standards," in *Temperature, Its Measurement and Control in Science and Industry*, C. M. Herzfeld, ed. (Reinhold, New York, 1962), Vol. 3, pp. 185-198.
8. K. D. Mielenz, R. D. Saunders, Jr., and J. B. Shumaker, "Spectroradiometric determination of the freezing temperature of gold," *J. Res. Natl. Inst. Stand. Technol.* **95**, 49-67 (1990).
9. H. Baker, ed., *American Society of Metals Handbook, Alloy Phase Diagrams* (ASM Materials Park, Ohio, 1992), Vol. 3, pp. 2:65-2:79.
10. O. Kubaschewski and C. B. Alcock, *Metallurgical Thermo-Chemistry* (Pergamon, New York, 1979), Chap. 1, p. 45.
11. T. J. Quinn, "The calculation of the emissivity of cylindrical cavities giving near blackbody radiation," *Br. J. Appl. Phys.* **18**, 1105-1113 (1967).
12. Y. S. Touloukian and D. P. DeWitt, eds., *Thermal Radiative Properties, Nonmetallic Solids* (IFI/Plenum, New York, 1972), Vol. 8, pp. 44-50.
13. T. Ricolfi and M. Battuello, "Precision infrared thermometer for the temperature interval $232^\circ\text{C} - 1085^\circ\text{C}$," in *Temperature, Its Measurement and Control in Science and Industry*, J. F. Schooley, ed. (American Institute of Physics, New York, 1992), Vol. 6, Part 2, pp. 797-800.